

A Robust Server-Effort Policy for Fluid Processing Networks

Harold Ship*, Evgeny Shindin†, Odellia Boni‡, Itai Dattner§

September 7, 2022

Abstract

Multi-Class Processing Networks describe a set of servers that perform multiple classes of jobs on different items. A useful and tractable way to find an optimal control for such a network is to approximate it by a fluid model, resulting in a Separated Continuous Linear Programming (SCLP) problem. Clearly, arrival and service rates in such systems suffer from inherent uncertainty. A recent study addressed this issue by formulating a Robust Counterpart for SCLP models with budgeted uncertainty which provides a solution in terms of processing rates. This solution is transformed into a sequencing policy. However, in cases where servers can process several jobs simultaneously, a sequencing policy cannot be implemented. In this paper, we propose to use in these cases a resource allocation policy, namely, the proportion of server effort per class. We formulate Robust Counterparts of both processing rates and server-effort uncertain models for four types of uncertainty sets: box, budgeted, one-sided budgeted, and polyhedral. We prove that server-effort model provides a better robust solution than any algebraic transformation of the robust solution of the processing rates model. Finally, to get a grasp of how much our new model improves over the processing rates robust model, we provide results of some numerical experiments.

1 Introduction

In multi-class processing networks *items* of different *types* arrive at the system, where they are processed in one or several ways, then follow individual paths through various *service stations*. Each service station can perform *jobs* of several different *classes*, such that each job processes items of a specific type. Once processed, items either change type or leave the system. To optimize system performance, one must control admissions, routing and sequencing of the items throughout the system [1], [2], [3], [4], [5], [6]. Such operational models are used in a number of applicative domains including manufacturing systems, multiprocessor computer systems, communication networks, data centers, and sensor networks. The straightforward formulation of such networks produces large stochastic dynamic programming problems that are computationally intractable. To overcome this, one can approximate the network with a fluid model. In order to find optimal solutions, we can formulate these networks as a specially structured class of continuous linear programs called Separated Continuous Linear Programs (SCLPs), which has been studied over the last few decades. Several algorithms

*Harold Ship is with the IBM Research - Haifa Lab, Haifa University Campus, Mount Carmel, Haifa 3490002, Israel and a PhD student at the University of Haifa. (e-mail: harold@il.ibm.com).

†Evgeny Shindin is with the IBM Research - Haifa Lab, Haifa University Campus, Mount Carmel, Haifa 3490002, Israel. (e-mail: evgensh@il.ibm.com).

‡Odellia Boni is with the IBM Research - Haifa Lab, Haifa University Campus, Mount Carmel, Haifa 3490002, Israel. (e-mail: odelliab@il.ibm.com).

§Itai Dattner is a Senior Lecturer at the University of Haifa Department of Statistics, University of Haifa, 199 Abba Khoushy, Haifa 3498838, Israel. (e-mail: idattner@stat.haifa.ac.il).

[7], [8], [9], [10], [11], [12], [13] have been developed to solve SCLPs and their generalizations. Some of these algorithms allow finding an exact solution. In particular, Weiss [10] developed the SCLP-simplex algorithm that provides an exact solution of SCLP problems in a finite bounded number of steps. Shindin and Weiss [14], [15], [12] extended this algorithm to more general M-CLP problems allows modeling impulse controls and solving general SCLP without additional assumption on the problem data. Shindin et al [13] provide an efficient implementation of the revised SCLP-simplex algorithm which finds exact solutions for SCLP problems with hundreds of servers and thousands of job classes in reasonable time. Nazarathy and Weiss [16] keep the deviations from the SCLP-generated model stable using a maximum pressure policy, which provide *stable* long-term solutions to fluid approximations to multi-class processing networks [17]

Clearly, in a real-life application the arrival and processing rates of the various items may be uncertain and, moreover can change over time. There are two possible treatments to address this problem:

- Stochastic fluid model considered by Cassandras et al [18] allows building gradient estimators of model parameters and then uses these estimators to build parameterized optimal control policies. This approach is mainly used for perturbation analysis and is computationally intractable for a large-scale processing networks.
- Robust optimization approach deals with uncertain model parameters residing in a bounded *uncertainty set* and optimizes against the worst-case realization of the parameters within this set. Robust optimization treats the uncertainty in a deterministic manner and produces a tractable representation of the uncertain problem known as *robust counterpart*. In the context of fluid models this approach was considered by Bertsimas et al. [19] who developed a robust counterpart for SCLP with a one-sided budgeted uncertainty set. The robust counterpart in [19] is also an SCLP problem and thus can be solved by the algorithms discussed earlier.

An important aspect of choosing a model formulation for a real-life problem is how to interpret its solution to a policy for the problem at hand. For example, for several types of processing networks, the model's solution should be transformed into a sequencing policy, namely, assigning priority to job classes so that when a server is done processing a job it will serve the next job from the class having highest priority. In the model suggested in [19], the system's control is formulated as processing rates for each job class. The resulting SCLP solution is used to assign priorities for the different job classes according to their processing rates at time $t = 0$. However, in cases where servers can process several jobs simultaneously, we do not face a sequencing problem, but a resource allocation problem, namely, how much of the server resources should be dedicated to each class. The idea of controlling the proportion of server effort in fluid models has been used by [20, 21]. In this paper we consider a *server-effort fluid model*, where the control is formulated in terms of proportion of the server resources dedicated to serving specific classes of jobs.

The contributions of the paper are as follows. (1) In Section 3.2 we derive robust counterparts for both processing-rates and server-effort controlled fluid models under the different uncertainty sets discussed in Section 2. (2) We compare the models under uncertainty and show that the server-effort model produces the same or better solution than the processing-rates model in Section 3.3. (3) We demonstrate the performance improvement using a numerical comparison of these models for a processing network which can be easily transformed between these models in Section 4.

2 Fluid Processing Networks

In what follows, we make several assumptions. First, we consider only networks where each job class j can be served by a single server denoted by $s(j)$, although each server can perform several classes of jobs. Second, all items of the specific type are stored in the dedicated buffer: when a job of a certain class is performed it takes an item from the buffer and the processed item either leaves the system or moves to another buffer for further processing. Therefore the arrival rate of a certain items is influenced by both the external arrival

rate and the processing rates of the servers. Finally, without loss of generality we also assume that buffer size is infinite. For the fluid approximation we consider fluids instead of individual items and flows instead of job classes.

2.1 Example: A Criss-Cross Network

Let us consider the Criss-Cross network presented in [19] and depicted in Figure 1. In this network we have three types of items which are processed by jobs of the corresponding classes, so that we have one-to-one correspondence between item types and job classes. This network comprises two servers: The first server, S_1 , contains two buffers B_1 and B_2 for items of types 1 and 2 respectively, that arrive from outside with rates λ_1, λ_2 . Once a class 1 job is complete, it produces an item of type 3 that enters the buffer B_3 on server S_2 . For each job class j , let μ_j be the maximal service rate in jobs per unit time if the corresponding server $s(j)$ processes this class at full capacity. At time t , $x_k(t)$ is the quantity of items in the buffer k .

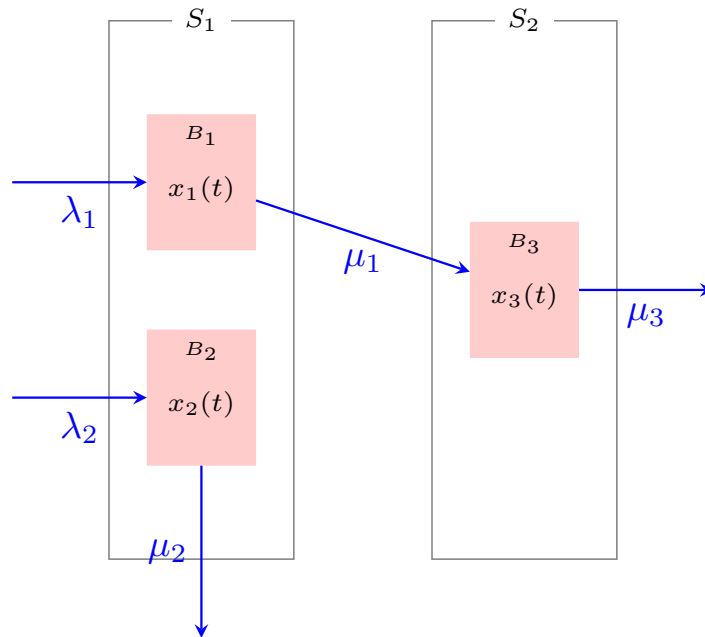


Figure 1: A Criss-cross network.

We formulate this queuing network as a fluid model by following: Let $\alpha_k = x_k(0)$ and λ_k be the initial amount of fluid and the exogenous arrival rate of the fluid to the buffer k respectively. Flow of class $j = k$ empties buffer k with maximum rate μ_j . Let $x_k(t)$ denote the total amount of fluid in the buffer k at time t . Here $x_k(t)$ are the system's state variables. The actual decision variables are the system's control variables relating to processing of different flows by the corresponding server.

There are two ways we can model this fluid network:

(A) We can control $u_j(t)$ - the actual processing rate of flow unit of class j per unit time at time t , so that

$0 \leq u_j(t) \leq \mu_j$. In this case the dynamics of the system can be expressed as:

$$\begin{aligned} x_1(t) &= \alpha_1 + \lambda_1 t - \int_0^t u_1(s) ds & \forall t, \\ x_2(t) &= \alpha_2 + \lambda_2 t - \int_0^t u_2(s) ds & \forall t, \\ x_3(t) &= \alpha_3 + \int_0^t u_1(s) ds - \int_0^t u_3(s) ds & \forall t, \end{aligned}$$

where the sum of the actual processing rates should not exceed the total server capacity:

$$\begin{aligned} \frac{u_1(t)}{\mu_1} + \frac{u_2(t)}{\mu_2} &\leq 1 & \forall t, \\ \frac{u_3(t)}{\mu_3} &\leq 1 & \forall t. \end{aligned}$$

(B) Alternatively, we can control $0 \leq \eta_j(t) \leq 1$ which is the dimensionless proportion of the server effort dedicated to flow j at time t . Clearly, the actual processing rates are proportional to the dedicated server efforts: $u_j(t) = \eta_j(t)\mu_j$. In this case the dynamics of the system can be expressed as:

$$\begin{aligned} x_1(t) &= \alpha_1 + \lambda_1 t - \int_0^t \mu_1 \eta_1(s) ds & \forall t, \\ x_2(t) &= \alpha_2 + \lambda_2 t - \int_0^t \mu_2 \eta_2(s) ds & \forall t, \\ x_3(t) &= \alpha_3 + \int_0^t \mu_1 \eta_1(s) ds - \int_0^t \mu_3 \eta_3(s) ds & \forall t, \end{aligned}$$

where the total server effort should not exceed 1:

$$\begin{aligned} \eta_1(t) + \eta_2(t) &\leq 1 & \forall t, \\ \eta_3(t) &\leq 1 & \forall t. \end{aligned}$$

2.2 General processing networks

Consider a processing network with I servers and J different job classes. We also have $k = 1, \dots, K$ buffers so that jobs of class j process items of type $k = k(j)$. Each job class j has an associated server $i = s(j)$ that processes jobs of this class. Items processed by the job class j routed to the buffer k with probability $p_{j,k}$ or leave the system with probability $1 - \sum_k p_{j,k}$.

In the associated fluid model the flow of class j empties buffer $k = k(j)$ and is processed by the server $i = s(j)$. After the processing fluid comes to the buffer l in proportion $p_{j,l}$ or leaves the system in proportion $1 - \sum_l p_{j,l}$. To simplify the notation we define matrix G of size $K \times J$ and set $G_{k,j} = 1$ for $k = k(j)$ and $G_{k,j} = -p_{j,k}$ for $k \neq k(j)$. We let λ_k be the rate of external arrivals to the buffer k and α_k be initial amount of fluid in the buffer k .

Let μ_j be the processing rate of flow j when the server devotes all of its effort to this flow, and $\tau_j = 1/\mu_j$ be mean service time per unit of flow j . Similarly to example in 2.1, for cost functions f, g on $\mathbb{R}^K, \mathbb{R}^J$ we can define two types of control policies:

(A) **Processing rates model** our decisions are actual processing rates $u_j(t) = \eta_j(t)\mu_j$. This is the approach taken in [19]. In this case the optimal control can be found by solving following optimization problem:

$$\begin{aligned} \min_{x(t), u(t)} & \int_0^T f(x(t)) + g(u(t)) dt, \\ \text{s.t.} & \int_0^t \sum_j G_{k,j} u_j(s) ds + x_k(t) = \alpha_k + \lambda_k t \quad \forall k, t, \end{aligned} \tag{1}$$

$$\begin{aligned} & \sum_{j: s(j)=i} \tau_j u_j(t) \leq 1 \quad \forall i, t, \\ & u(t), x(t) \geq 0. \end{aligned} \tag{2}$$

(B) **Server-effort model** our decisions are proportions of the server effort $\eta_j(t)$. In this case the optimal control can be found by solving following optimization problem, where \circ denotes elementwise multiplication:

$$\begin{aligned} \min_{x(t), \eta(t)} & \int_0^T f(x(t)) + g(\mu \circ \eta(t)) dt, \\ \text{s.t.} & \int_0^t \sum_j G_{k,j} \mu_j \eta_j(s) ds + x_k(t) = \alpha_k + \lambda_k t \quad \forall k, t, \end{aligned} \quad (3)$$

$$\begin{aligned} & \sum_{j:s(j)=i} \eta_j(t) \leq 1 \quad \forall i, t, \\ & \eta(t), x(t) \geq 0. \end{aligned} \quad (4)$$

One can see that these models are interchangeable, meaning that optimal solutions can be obtained each from other by substituting $\eta_j(t) = \tau_j u_j(t) \quad \forall j$, or $u_j(t) = \mu_j \eta_j(t) \quad \forall j$. In the next section we show that the equivalence between solutions the models holds only for the case when service rates are certain.

3 Fluid Processing Networks under Uncertainty

3.1 Modelling Uncertainty

In practice arrival rates λ_k , service rates μ_j , and/or mean service times $\tau_j = 1/\mu_j$ can be uncertain, meaning that we do not know their exact values at optimization time. Moreover these parameters can also change over time. We assume that the unknown parameters belong to some bounded uncertainty set \mathcal{U} . The uncertainty set is assumed to be known (or estimated from historical data) a priori.

For a given uncertainty set \mathcal{U} , one can define a new optimization problem whose solution is feasible under all possible realizations of the uncertain parameters. Such a problem is known as the *robust counterpart*. The formulation of the robust counterpart depends both on the initial problem and the the uncertainty set. The robust approach is conservative in that it protects against the worst-case scenario. It should be noted that a robust counterpart is created per constraint, so constraints are treated individually even if the same uncertain parameters are shared between them. This is conservative because the worst-case scenario for one constraint can be different than for another.

Let us denote all uncertain time-varying parameters of a problem by $\theta_\ell(t), \ell = 1, \dots, L$. We formulate each of these parameters as $\theta_\ell(t) = \bar{\theta}_\ell + \tilde{\theta}_\ell \zeta_\ell(t)$ where $\bar{\theta}_\ell$ is called the *nominal* value of the uncertain parameter $\theta_\ell(t)$, $\tilde{\theta}_\ell$ denotes the maximal *deviation* of $\bar{\theta}_\ell$ from its nominal value, and $\zeta_\ell(t)$ is called the *perturbation*. To keep robust counterpart simple and computationally tractable we model uncertainty using one of the following uncertainty sets:

- *Box uncertainty set.* The perturbations affecting the uncertain parameters reside in a box : $|\zeta_\ell(t)| \leq 1 \forall t, \ell = 1, \dots, L$. This means that $\theta_\ell(t)$ can take values in the interval $[\bar{\theta}_\ell - \tilde{\theta}_\ell, \bar{\theta}_\ell + \tilde{\theta}_\ell]$. Such a set indicates that the perturbations are independent of each other.
- *Budgeted uncertainty set.* Consider, that in addition to the box uncertainty for some group of parameters \mathbb{L} we have an additional restriction on the total magnitude of the perturbations: $\sum_{\ell \in \mathbb{L}} |\zeta_\ell(t)| \leq \Gamma$. When $\Gamma \leq \|\mathbb{L}\|$ is called the uncertainty budget. As robust counterpart is formulated per constraint, the uncertainty budget also refers to the specific constraint and refers to the uncertain parameters related to this constraint.
- *Budgeted one-sided uncertainty set.* Similar to the budgeted uncertainty set, but here one consider only positive perturbations $0 \leq \zeta_\ell(t) \leq 1 \forall t$ and restrict on the total sum by: $\sum_{\ell \in \mathbb{L}} \zeta_\ell(t) \leq \Gamma$.

- *Polyhedral uncertainty set.* The perturbations reside in a polyhedron, meaning $\{\zeta(t) | D\zeta(t) + d \geq 0\} \forall t$, where $D \in R^{M \times L}$ and $d \in R^M$ for some $M > 0$.

Note that level of conservativeness of the robust counterpart depends on the volume of the uncertainty set. Thus, in general, it is desirable to use a smaller uncertainty set.

The uncertain parameters referring to arrival rates λ_k appear in both processing rates model and server-effort model. The other uncertain parameters vary between the models: processing rates model is affected by uncertainty in mean service time per flow unit $\tau_j(t) = \bar{\tau}_j + \tilde{\tau}_j \zeta_j(t)$, while in server-effort model the uncertain parameters are service rate flow per unit time $\mu_j(t) = \bar{\mu}_j - \tilde{\mu}_j \zeta_j(t)$. Since $\tau_j = 1/\mu_j$, the shape of the uncertainty set affecting τ_j may vary from the shape of the uncertainty set affecting μ_j . Moreover, those parameters in different models are related to the different constraints and hence, even though in their deterministic form processing rates model and server-effort model are equivalent, their robust counterparts, and therefore the solutions they yield, may differ.

3.2 Robust counterparts

As mentioned in Section 3.1 formulation of a robust counterpart of an uncertain constraint depends both on the original constraint and on the shape of the uncertainty set its uncertain parameters reside in. In this section we present tractable robust counterparts for the different constraints of the processing rates model and the server-effort model for the uncertainty sets described in Section 3.1. Proofs of the propositions below can be found in the Appendix.

As the robust counterpart is formulated per constraint, we consider the uncertainty set affecting the uncertain parameters for each constraint individually. Therefore, for system dynamics constraints in the processing rates model (Equation (1)) which contain only a single uncertain parameter - arrival rate λ_k , all uncertainty sets are equivalent to a box uncertainty, resulting in the same robust counterpart:

Proposition 1. *The robust counterpart of Equation (1) for all uncertainty sets shapes is*

$$\alpha_k + (\bar{\lambda}_k - \tilde{\lambda}_k)t - \sum_j \int_0^t G_{kj} u_j(s) ds \geq 0, \forall k, t. \quad (5)$$

For server capacity constraints in processing rates model the uncertain parameters are mean service time per flow unit τ_j related to all flows processing by server $s(j)$.

Proposition 2. *The robust counterparts of Equation (2) are given in Table 1.*

For the server-effort model the uncertain parameters in each of the constraints (3) are service rates per unit time of all related flows μ_j and also exogenous arrival rate λ_k , while there is no uncertainty affecting Equation (4).

Proposition 3. *The robust counterparts of Equation (3) are given in Table 2.*

The objective functionals also depend on uncertain parameters, and thus their robust counterparts should be built w.r.t a specific $f(\cdot), g(\cdot)$ and specific uncertainty set. In the special case, where the objective is to minimize holding costs in the buffers we have $f(x(t)) = c^\top x(t)$ and $g(u(t)) = 0$. In this case the robust counterparts of the objective has shape of SCLP objective and hence resulting problem is tractable. Substituting the system dynamic equations (1) or (3) into the objective, one can see that value of the objective functional depends on uncertainty in arrival rates λ . However, as cost related to the arrival rates independent of our control it is possible to calculate the maximal arrival cost A independently from the optimization of the fluid model as specified in Table 3.

Uncertainty set	Robust Counterpart
Box	$\sum_{j:s(j)=i} (\bar{\tau}_j + \tilde{\tau}_j) u_j(t) \leq 1$
One-sided & Budgeted	$\Gamma_i \beta_i(t) + \sum_{j:s(j)=i} (\bar{\tau}_j u_j(t) + \gamma_j(t)) \leq 1,$ $\beta_i(t) + \gamma_j(t) - u_i(t) \tilde{\tau}_i \geq 0, \quad j = 1, \dots, J$ $\beta(t), \gamma(t) \geq 0$
Polyhedral	$\sum_j \bar{\tau}_j u_j(t) - \sum_m \delta_m(t) d_m \leq 1,$ $\sum_m D_{mj} \delta_m = u_j(t) \tilde{\tau}_j, \quad j = 1, \dots, J, \quad \delta \geq 0.$

Table 1: Processing rates model: Robust counterpart to server capacity constraints Equation (2)

Uncertainty set	Robust Counterpart
Box	$\alpha_k + (\bar{\lambda}_k - \tilde{\lambda}_k)t - \sum_{j:k(j)=k} \int_0^t (\bar{\mu}_j + \tilde{\mu}_j) \eta_j(s) ds + \sum_{j:k(j) \neq k} \int_0^t G_{kj} (\bar{\mu}_j - \tilde{\mu}_j) \eta_j(s) ds \geq 0$
One-sided	$\alpha_k + (\bar{\lambda}_k - \tilde{\lambda}_k)t - \sum_j G_{kj} \bar{\mu}_j \int_0^t \eta_j(s) ds + \sum_i \Gamma_i \beta_{ki}(t) + \sum_i \sum_{j:s(j)=i} \gamma_{kij}(t) \geq 0$ $\gamma_{kij}(t) + \beta_{ki}(t) \geq -G_{kj} \tilde{\mu}_j \int_0^t \eta_j(s) ds \quad \forall (i, j : s(j) = i), \quad \gamma(t), \beta(t) \geq 0$
Budgeted	$\alpha_k + (\bar{\lambda}_k - \tilde{\lambda}_k)t - \sum_j G_{kj} \bar{\mu}_j \int_0^t \eta_j(s) ds + \sum_i \Gamma_i \beta_{ki}(t) + \sum_i \sum_{j:s(j)=i} \gamma_{kij}(t) \geq 0$ $\beta_{ki}(t) + \gamma_{kij}(t) - 2\tilde{\delta}_{kij} \geq -G_{kj} \tilde{\mu}_j \int_0^t \eta_j(s) ds,$ $\delta_{kij}(t) + G_{kj} \tilde{\mu}_j \int_0^t \eta_j(s) ds \geq 0 \quad \forall (i, j : s(j) = i), \quad \gamma(t), \delta(t), \beta(t) \geq 0$
Polyhedral	$\alpha_k + (\bar{\lambda}_k - \tilde{\lambda}_k)t - \sum_j G_{kj} \bar{\mu}_j \int_0^t \eta_j(s) ds + \sum_m d_m \delta_{km}(t) \geq 0$ $- \sum_m D_{mj} \delta_{km} = G_{kj} \tilde{\mu}_j \int_0^t \eta_j(s) ds \quad \forall j, \quad \delta(t) \geq 0$

Table 2: Server-effort model: Robust counterpart to system dynamics constraints Equation (3)

Proposition 4. Let $f(x(t)) = c^\top x(t), c \geq 0$, $g(u(t)) = 0$ and Λ taken from Table 3 then the robust counterpart of objective functional for processing rates model is equivalent to:

$$\begin{aligned} \min_{u(t), z(t)} \quad & \int_0^T z(t) dt \\ \text{s.t.} \quad & At + c^\top \alpha - \int_0^t c^\top G u(s) ds \leq z(t), \forall t, \end{aligned} \quad (6)$$

Uncertainty set	Maximal arrival cost Λ
Box	$\Lambda = c^\top(\bar{\lambda} + \tilde{\lambda})$
One-sided & Budgeted	$\Lambda = c^\top \bar{\lambda} + \min_{\beta^*, \gamma^*} \Gamma^* \beta^* + \sum_k \gamma_k^*$ $\beta^* + \gamma_k^* - c_k \tilde{\lambda}_k \geq 0, k = 1, \dots, K, \beta^*, \gamma^* \geq 0$
Polyhedral	$\Lambda = c^\top \bar{\lambda} - \max_{\delta^*} \sum_m \delta_m^* d_m,$ $D^\top \delta^* = -c_k \tilde{\lambda}_k, k = 1, \dots, K, \delta^* \geq 0$

Table 3: Robust arrival rates

Uncertainty	Robust Counterpart
Box	$z(t) \geq At + \sum_k c_k \left[\alpha_k - \sum_{j:k(j)=k} \int_0^t (\bar{\mu}_j - \tilde{\mu}_j) \eta_j(s) ds + \sum_{j:k(j) \neq k} \int_0^t G_{kj} (\bar{\mu}_j + \tilde{\mu}_j) \eta_j(s) ds \right]$
One-sided	$z(t) \geq At + \sum_k c_k \left[\alpha_k - \int_0^t \sum_j G_{kj} \bar{\mu}_j \eta_j(s) ds + \sum_i \Gamma_i \beta_{ki}(t) + \sum_i \sum_{j:s(j)=i} \gamma_{kij}(t) \right]$ $\gamma_{kij}(t) + \beta_{ki}(t) \geq G_{kj} \tilde{\mu}_j \int_0^t \eta_j(s) ds \forall (i, j : s(j) = i), \gamma_{kij}(t), \beta_{ki}(t) \geq 0$
Budgeted	$z(t) \geq At + \sum_k c_k \left[\alpha_k - \int_0^t \sum_j G_{kj} \bar{\mu}_j \eta_j(s) ds + \sum_i \Gamma_i \beta_{ki}(t) + \sum_i \sum_{j:s(j)=i} \gamma_{kij}(t) \right]$ $\beta_{ki}(t) + \gamma_{kij}(t) - 2\delta_{kij} \geq G_{kj} \tilde{\mu}_j \int_0^t \eta_j(s) ds,$ $\delta_{kij}(t) - G_{kj} \tilde{\mu}_j \int_0^t \eta_j(s) ds \geq 0 \forall (i, j : s(j) = i), \gamma(t), \delta(t), \beta(t) \geq 0$
Polyhedral	$z(t) \geq At + \sum_k c_k \left[\alpha_k - \int_0^t \sum_j G_{kj} \bar{\mu}_j \eta_j(s) ds - \sum_m d_m \delta_{km}(t) \right]$ $\sum_m D_{mj} \delta_{km} = G_{kj} \tilde{\mu}_j \int_0^t \eta_j(s) ds \forall j, \delta(t) \geq 0$

Table 4: Robust objective functions for server-effort model

Proposition 5. Let $f(x(t)) = c^\top x(t), c \geq 0$, $g(u(t)) = 0$ then the robust counterpart of objective functional

for server-effort model is equivalent to:

$$\min_{\eta(t), z(t)} \int_0^T z(t) dt$$

s.t. Constraints: (Table 4)

The proofs of Proposition 4 and Proposition 5 are very similar to those of Proposition 1 and Proposition 3, respectively.

Based on Propositions 1, 2 and 4 the robust counterpart of processing rates model is:

$$\min_{u(t), z(t)} \int_0^T z(t) dt$$

s.t. Constraints: Equations (5) and (6), Table 1,

$$u(t) \geq 0, \tag{7}$$

Based on Propositions 3 and 5 the robust counterpart of server-effort model is:

$$\min_{\eta(t), z(t)} \int_0^T z(t) dt$$

s.t. Constraints: Tables 2 and 4, Eq. 4,

$$\eta(t) \geq 0 \tag{8}$$

3.3 Processing-rates model vs Server-effort model

The processing rates model represents a case where the suitable control of the system at hand is its class specific processing rates $u_j(t)$ while the server-effort model is used to describe cases where system is controlled by the proportion of resources dedicated to specific job classes $\eta_j(t)$. When no uncertainty affects the models, they are equivalent. In other words, any solution of the processing rates model can be transformed into a solution of the server-effort model using the relation $\eta(t) = \tau(t)u(t)$. In particular, if $u_j^*(t)$ is an optimal solution for the processing rates model, then $\eta^*(t) = \tau(t)u_j^*(t)$ is an optimal solution for the server-effort model. When uncertainty is introduced into the models, this is no longer possible in general. If $u_j(t)$ is a robust solution for the processing rates model (e.g. of Problem (7)), then the value of $\eta(t) = \tau(t)u(t)$ depends on the uncertain parameters $\tau_j(t)$. However, we need a certain and feasible transformation to implement this solution as a control for the server-effort model ((e.g. of Problem (8)). This applies also to the robust optimal solutions of the models.

Let us assume there exists a transformation $h : u(t) \rightarrow \eta(t)$ between robust solutions of processing rates model and server-effort model. That is to say, if $u(t)$ is a feasible solution of Problem (7), then $h : u(t) \rightarrow \eta(t)$ is a feasible solution of Problem (8)). In the following theorem we show that a robust optimal solution of server-effort model is as good or better than any such transformation $h(u)$ of the robust optimal solution of processing rates model.

Theorem 6. *Let $u^*(t)$ be an optimal solution of Problem (7). Let h be a transformation from the solution space of Problem (7) to the solutions space of Problem (8), and let $\eta^*(t) = h(u^*(t))$. Then the optimal objective value of Problem (8) is at least as good as that of $\eta^*(t)$.*

Proof. $\eta^*(t) = h(u^*(t))$ where $u^*(t)$ is the optimal solution of Problem (7), must be a feasible solution of Problem (7). However, it is not necessarily optimal. □

Note that Theorem 6 applies to all uncertainty sets and objective functionals.

4 Computational Results

Theorem 6 indicates that the optimal robust solution of the server-effort model is as good or better than the transformed optimal robust solution of processing rates model. In this section we perform a numerical study on two example systems to quantify how much optimal robust solution of server-effort model outperforms the transformed optimal robust solution of processing rates model in terms of holding cost. These systems have 10 and 20 servers respectively, with 10 job classes processed on each server and no internal inflows in order to have straightforward transformation rules. The two models being compared handle uncertainty in arrival rates in the same manner, Therefore we opted to simplify our example by looking only at uncertain service times $\tau(t)$. We consider a box uncertainty set $\tau(t) = \bar{\tau} + \epsilon\bar{\tau}\zeta(t)$ where ϵ denotes the maximal deviation of actual service time $\tau(t)$ from its nominal value $\bar{\tau}$. Now $\mu(t) = 1/\tau(t)$, so $\frac{1}{(1+\epsilon)\bar{\tau}_j} \leq \mu_j(t) \leq \frac{1}{(1-\epsilon)\bar{\tau}_j}$. Solving for the midpoint of this box gives us the equivalent uncertainty set $\bar{\mu} - \epsilon\bar{\mu}\zeta(t)$ centered around $\bar{\mu}_j = \frac{1}{\bar{\tau}_j(1-\epsilon^2)}$.

Parameter values for the example system are taken randomly from the values in Table 5.

Name	Symbol	Range
nominal service rate	$\bar{\mu}_j = 1/\bar{\tau}_j$	5 - 25
nominal arrival rate	λ_k	2 - 5
initial buffer size	α_k	10 - 20
holding cost	c_k	1 - 2

Table 5: Experimental parameters used in simulations. Values were randomly sampled from the given range.

The general approach is to construct the robust counterparts for both a processing rates model and a server-effort model (meaning, Problems (7), (8) respectively) for the same randomized set of parameters $\tau = 1/\mu, \lambda, \alpha, c$. Next, we solve these two SCLP problems to obtain their optimal robust controls $u^*(t)$ and $\eta^*(t)$. We then create ten realizations of $\tau(t) = [\tau_1(t), \dots, \tau_K(t)]$ using Equation (9) for each of the ten sets of random model parameters, for a total of 100 realizations of $\tau(t)$. Figure 2 depicts several examples of such realizations.

$$\tau_k(t) = \tau_k + \frac{1}{4} \sum_{n=1}^4 \sin(n\pi t + \phi_n), \quad \phi_n \sim U[0, 2\pi] \quad (9)$$

For each realization, we can compute the actual buffer sizes $x_k(t)$ in the system when applying the robust optimal control $\eta^*(t)$ and their sizes when applying the transformed control $\eta_j^u(t) = u_j^*(t)/(1 - \tau_j)$.

These actual buffer sizes determine the actual holding cost for both these controls. Lastly, we average the difference between those objective values over all 100 realizations. We repeat this procedure ten times, each time using a new set of random parameters, and compute the average difference between objective values over the ten parameters sets.

We ran this experiment for two different sized networks: a) a smaller network with $I = 10$ servers and $J = 100$ job classes, and b) a larger network with $I = 20$ servers and $J = 200$ job classes. In both cases, the networks have no internal inflows, meaning that $J = K$ and $G_{kj} = 0$ when $j \neq k$. For each of network, we ran the experiment for five values of relative uncertainty: $\epsilon \in \{0.01, 0.02, 0.05, 0.1, 0.2\}$. Algorithm 1 describes in detail the experimental flow.

Results, which are summarized in Table 6 indicate that the relative improvement of robust control of server-effort model over control derived from robust control of processing rates model increases with the level of uncertainty. The results also suggest that this improvement size is independent of network size. *Note:* The computational costs of the the new model will be explored in a subsequent paper. The python code for running the experiments can be found in [22], a fork of [23].

Algorithm 1 Method for numerical experiment

Require: I, J, K, ϵ

```
for  $n_p = 1, \dots, 10$  do ▷ random models  
  random  $\tau = 1/\mu, \lambda, \alpha, c$  ▷ from Table 5  
   $u^*(t) \leftarrow$  processing rates model using  $(1 + \epsilon)\tau$  ▷ from Table 1  
  
   $\eta^*(t) \leftarrow$  server-effort model using  $[\tau(1 - \epsilon)]^{-1}$  ▷ worst case of  $\mu$  for  $\tau(t) \geq (1 - \epsilon)\tau$   
  
  for  $n_t = 1, \dots, 10$  do ▷ perturbations of  $\tau$   
     $\tau(t) \leftarrow \text{rand}(\tau)$  ▷ explained below  
    Processing rates model:  
     $\eta^u(t) \leftarrow u^*(t)\tau(1 - \epsilon)$  ▷ transformation of  $u^*(t)$   
     $\hat{x}_1 \leftarrow \alpha + \lambda t - \int_0^t \eta^u(s)/\tau(s) ds$   
     $z_1 \leftarrow \int_0^T c^\top \hat{x}_1(t) dt$   
    Server-effort model:  
     $\hat{x}_2 \leftarrow \alpha + \lambda t - \int_0^t \eta^*(s)/\tau(s) ds$   
     $z_2 \leftarrow \int_0^T c^\top \hat{x}_2(t) dt$   
    Relative difference:  
     $\Delta_{12} \leftarrow (z_1 - z_2)/z_1$  ▷ relative difference  
  end for  
end for
```

5 Discussion and Conclusion

5.1 Discussion

In this research we have elicited a new robust model for Fluid Processing Network problems with control over the proportion of server-effort dedicated to serving different flows. Our primary contribution is to prove that this model is better than the transformed processing rates model of [19] for networks whose control is the proportion of server effort on each class.

Our second contribution is extending both models to cover box, budgeted, one-sided budgeted and polyhedral uncertainty sets. These shapes have the advantage that they are less conservative than box uncertainty. Robust optimization problems with budgeted uncertainty occur frequently, since there may be interdependence between parameter values. Uncertainty set modeling may be based on observed values of the uncertain parameters. In this case, one may decide to model the uncertainty set as the convex hull of

ϵ	Improvement Δ_{12} (%)	ϵ	Improvement Δ_{12} (%)
0.01	1.42	0.01	1.47
0.02	2.93	0.02	2.89
0.05	6.76	0.05	6.91
0.10	11.76	0.10	12.04
0.20	19.56	0.20	19.29

(a) For 10 servers, 100 flows (b) For 20 servers, 200 flows

Table 6: Mean relative percent improvement of the server-effort model model over the processing rates model.

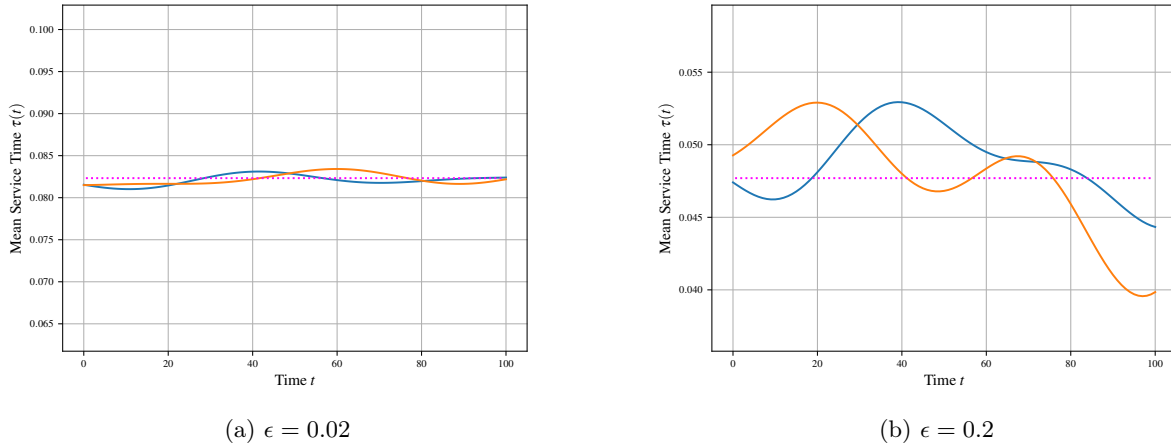


Figure 2: Examples of realizations of $\tau(t)$ for different values of ϵ . Dotted lines indicate value of τ .

these observations, which corresponds to polyhedral uncertainty.

Finally, our third contribution is to quantitatively demonstrate, using numerical experiments, how our new model outperforms the current processing rates model of [19] for server-effort controls. In our experiments, the relative improvement of our model increased with the magnitude of the uncertainty, although we did not see any difference for models of different sizes.

5.2 Limitations

While our model improves on the processing rates model when control is over server effort, it does not generalize to standard fluid processing networks, where the rates of flow are under control so the model of [19] is more natural. Our computational results covered a limited subset of possible fluid processing networks, in particular those for which the actual controls are server-effort proportion. Next, while we were able to formulate tractable robust counterparts for several classes of uncertainty sets, there are other useful types of uncertainty sets which we did not handle. Bertsimas, Brown and Caramanis [24] describe ellipsoidal, cardinality constrained, and general norm uncertainty sets, for which we know of no robust formulation of SCLP. Lorca and Sun [25] describe dynamic uncertainty sets which are not supported by the SCLP-simplex algorithm which currently supports only a constant matrix. Finally, our computational results covered only box uncertainty sets. This is due to a limitation in the solver [23] in handling degenerate problems.

5.3 Future work

In this paper, we assume that uncertainty set of our robust model is known. We would like to study the statistical properties of the network state and controls by considering the stochastic nature of the uncertain parameters estimation. The solver [23] used in this work does not handle degenerate problems. We would like to extend this solver to handle degenerate problems to solve robust counterparts of problems with additional shapes of uncertainty sets. In this paper, we solved robust SCLP problems with constant arrival and service rates. We plan to extend the theory of SCLP and the solver [23] to include piece-wise constant rates.

References

- [1] J. M. Harrison, “Brownian models of queueing networks with heterogeneous customer populations,” in *Stochastic differential systems, stochastic control theory and applications*. Springer, 1988, pp. 147–186.
- [2] L. M. Wein, “Scheduling networks of queues: heavy traffic analysis of a multistation network with controllable inputs,” *Oper. Research*, vol. 40, no. 3-suppl-2, pp. S312–S334, 1992.
- [3] F. Kelly and C. Laws, “Dynamic routing in open queueing networks: Brownian models, cut constraints and resource pooling,” *Queueing systems*, vol. 13, no. 1-3, pp. 47–86, 1993.
- [4] J. G. Dai, “On positive harris recurrence of multiclass queueing networks: a unified approach via fluid limit models,” *The Annals of Applied Probability*, pp. 49–77, 1995.
- [5] M. Bramson, *Stability of queueing networks*. Springer, 2008.
- [6] S. Meyn, *Control techniques for complex networks*. Cambridge University Press, 2008.
- [7] M. C. Pullan, “An algorithm for a class of continuous linear programs,” *SIAM J. on Control and Optimization*, vol. 31, no. 6, pp. 1558–1577, 1993.
- [8] X. Luo and D. Bertsimas, “A new algorithm for state-constrained separated continuous linear programs,” *SIAM J. on control and optimization*, vol. 37, no. 1, pp. 177–210, 1998.
- [9] L. Fleischer and J. Sethuraman, “Efficient algorithms for separated continuous linear programs: the multicommodity flow problem with holding costs and extensions,” *Math. of Oper. Research*, vol. 30, no. 4, pp. 916–938, 2005.
- [10] G. Weiss, “A simplex based algorithm to solve separated continuous linear programs,” *Mathematical Programming*, vol. 115, no. 1, pp. 151–198, 2008.
- [11] D. Bampou and D. Kuhn, “Polynomial approximations for continuous linear programs,” *SIAM J. on Optimization*, vol. 22, no. 2, pp. 628–648, 2012.
- [12] E. Shindin and G. Weiss, “A simplex-type algorithm for continuous linear programs with constant coefficients,” *Mathematical Programming*, pp. 1–45, 2018.
- [13] E. Shindin, M. Masin, G. Weiss, and A. Zadorojniy, “Revised scip-simplex algorithm with application to large-scale fluid processing networks,” in *2021 60th IEEE Conference on Decision and Control (CDC)*, 2021, pp. 3863–3868.
- [14] E. Shindin and G. Weiss, “Symmetric strong duality for a class of continuous linear programs with constant coefficients,” *SIAM J. on Optimization*, vol. 24, no. 3, pp. 1102–1121, 2014.
- [15] —, “Structure of solutions for continuous linear programs with constant coefficients,” *SIAM J. on Optimization*, vol. 25, no. 3, pp. 1276–1297, 2015.
- [16] Y. Nazarathy and G. Weiss, “Near optimal control of queueing networks over a finite time horizon,” *Annals of Oper. Research*, vol. 170, no. 1, p. 233, 2009.
- [17] J. G. Dai and W. Lin, “Maximum pressure policies in stochastic processing networks,” *Oper. Research*, vol. 53, no. 2, pp. 197–218, 2005.

- [18] C. Cassandras, Y. Wardi, B. Melamed, G. Sun, and C. Panayiotou, "Perturbation analysis for online control and optimization of stochastic fluid models," *IEEE Transactions on Automatic Control*, vol. 47, no. 8, pp. 1234–1248, 2002.
- [19] D. Bertsimas, E. Nasrabadi, and I. C. Paschalidis, "Robust fluid processing networks," *IEEE Transactions on Automatic Control*, vol. 60, no. 3, pp. 715–728, 2014.
- [20] M. Bramson, "Convergence to equilibria for fluid models of head-of-the-line proportional processor sharing queueing networks," *Queueing Systems*, vol. 23, no. 1, p. 1–26, 1996.
- [21] —, "State space collapse with application to heavy traffic limits for multiclass queueing networks," *Queueing Systems*, vol. 30, no. 1, p. 89–140, Nov 1998.
- [22] E. Shindin and H. Ship, "SCLP-Python," 3 2022. [Online]. Available: <https://github.com/haroldship/SCLP solver>
- [23] E. Shindin, "SCLP-Python," 7 2021. [Online]. Available: <https://github.com/IBM/SCLP solver>
- [24] D. Bertsimas, D. B. Brown, and C. Caramanis, "Theory and applications of robust optimization," *SIAM Review*, vol. 53, no. 3, p. 464–501, Jan 2011.
- [25] A. Lorca and X. A. Sun, "Adaptive robust optimization with dynamic uncertainty sets for multi-period economic dispatch under significant wind," *IEEE Transactions on Power Systems*, vol. 30, no. 4, p. 1702–1713, Jul 2015.
- [26] A. Ben-Tal, L. El Ghaoui, and A. Nemirovski, *Robust Optimization*. Princeton University Press, Aug. 2009.

A Proofs

Proposition 1. For all mentioned uncertainty shapes, we note that each individual system dynamics constraint contains only single uncertain parameter, so all uncertainty sets could be considered as box uncertainty related to this parameter. For any buffer k and for every realization of ξ , the balance constraint (1) is:

$$\alpha_k + \left(\bar{\lambda}_k + \tilde{\lambda}_k \xi_k(t)\right) t - \sum_j \int_0^t G_{kj} u_j(s) ds \geq 0 \quad \forall t. \quad (10)$$

We are going to express Equation (10) in terms of fixed parameters, while including all cases of uncertainty. For box uncertainty, $|\xi_k(t)| \leq 1$ means that $\bar{\lambda}_k + \tilde{\lambda}_k \xi_k(t) \geq \bar{\lambda}_k - \tilde{\lambda}_k \quad \forall t$. So the reformulated constraint

$$\alpha_k + \left(\bar{\lambda}_k - \tilde{\lambda}_k\right) t + \sum_j \int_0^t G_{kj} u_j(s) ds \geq 0 \quad \forall t, k.$$

covers all realizations of uncertainty. □

Proposition 2. For box uncertainty, $|\zeta_j(t)| \leq 1 \quad \forall t, i$ implies that $(\bar{\tau}_j + \tilde{\tau}_j \zeta_j(t)) \leq (\bar{\tau}_j + \tilde{\tau}_j) \quad \forall t, j$ and hence the robust counterparts of Equation (2) is:

$$\sum_{j:s(j)=i} (\bar{\tau}_j + \tilde{\tau}_j) u_j(t) \leq 1$$

The proof for the one-sided budgeted uncertainty can be found in [19, Theorem 1]. For the other types of uncertainty, we also follow the method of proof of [19, Theorem 1]. The uncertain server capacity constraints (2), must hold for all realizations of $\zeta(t)$ within uncertainty set. In particular, for any $\zeta(t)$ that maximizes LHS of these constraints. This introduces linear programming (LP) problems, for each server i and for each t .

For budgeted uncertainty set it can be expressed by:

$$\begin{aligned} \max_{\zeta(t)} \quad & \sum_{j:s(j)=i} (\bar{\tau}_j + \zeta_j(t)\tilde{\tau}_j) u_j(t) \\ \text{s.t.} \quad & \sum_{j:s(j)=i} |\zeta_j(t)| \leq \Gamma_i, \quad |\zeta_j(t)| \leq 1. \end{aligned} \quad (11)$$

To find the dual of (11), we note that $\sum |\zeta_j(t)| \leq \Gamma_i$ is equivalent to the system $-w_j(t) \leq \zeta_j(t) \leq w_j(t)$, $\sum w_j(t) \leq \Gamma_i$, $w_j(t) \leq 1$, $w_j(t) \geq 0$. With this, we can consider our problem a lower-dimensional representation of a LP with added variables w_j , $j = 1, \dots, J$ [26, Section 1.3]. Considering Lagrange multipliers $\beta_i(t)$, $\gamma_j(t)$, $\phi_j(t)$, $\nu_j(t)$, we derive the dual:

$$\begin{aligned} \min_{\beta(t), \gamma(t)} \quad & \Gamma_i \beta_i(t) + \sum_{j:s(j)=i} (\bar{\tau}_j u_j(t) + \gamma_j(t)) \\ \text{s.t.} \quad & -\phi_j(t) - \nu_j(t) + \beta_i(t) + \gamma_j(t) \geq 0, \\ & \phi_j(t) - \nu_j(t) = \tilde{\tau}_j(t) u_j(t), \\ & \beta_i(t), \gamma_j(t), \phi_j(t), \nu_j(t) \geq 0, \text{ for } s(j) = i. \end{aligned}$$

Furthermore, since $\tilde{\tau}_j(t) u_j(t) \geq 0$, we can set $\nu_j(t) = 0$ and hence problem could be reduced to:

$$\begin{aligned} \min_{\beta(t), \gamma(t)} \quad & \Gamma_i \beta_i(t) + \sum_{j:s(j)=i} (\bar{\tau}_j u_j(t) + \gamma_j(t)) \\ \text{s.t.} \quad & \beta_i(t) + \gamma_j(t) \geq \tilde{\tau}_j(t) u_j(t), \\ & \beta_i(t), \gamma_j(t) \geq 0, \text{ for } s(j) = i. \end{aligned}$$

For polyhedral uncertainty $D\zeta(t) + d \geq 0$ where $D \in \mathbb{R}^{M \times J}$ and $d \in \mathbb{R}^M$, we similarly derive the following dual problem from which the constraints in Table 1 are derived:

$$\begin{aligned} \min_{\delta(t)} \quad & -\sum_m d_m \delta_m(t) \\ \text{s.t.} \quad & \sum_m D_{mj} \delta_m(t) = u_j(t) \tilde{\tau}_j, \quad \delta(t) \geq 0. \end{aligned}$$

These dual problems are equivalent to the constraints in Table 1. \square

Proposition 3. For all realizations of uncertainty and all t, k, j , we have $\bar{\lambda}_k - \tilde{\lambda}_k \leq \bar{\lambda}_k + \tilde{\lambda}_k \xi_k(t) \leq \bar{\lambda}_k + \tilde{\lambda}_k$, and $\bar{\mu}_j - \tilde{\mu}_j \leq \bar{\mu}_j + \tilde{\mu}_j \zeta_j(t) \leq \bar{\mu}_j + \tilde{\mu}_j$. Our constraint must hold for all values of uncertain parameters, in particular those that minimize the buffer quantity. The result for box uncertainty is therefore clear.

For the other types of uncertainty, let S be the compact set of possible values of $\zeta(s)$. Then we can exchange the order of integration and maximization. Furthermore, $\max_{s \in S} \zeta(s) = \max \zeta(t)$ and since G_{kj} and $\tilde{\mu}_j$ are constants, and $\eta_j(s) \geq 0$, we can extract $\zeta_j(s)$ from inside the integral to $\zeta_j(t)$ outside, and we our constraint is now a linear function of $\zeta_j(t)$, $j = 1, \dots, J$.

For one-sided budgeted uncertainty, we note that for inflows, the minimum occurs when $\zeta_j(t) = 0$. Taking the maximum to be the negative of the minimum, we derive a separate LP subproblem for each server i :

$$\begin{aligned} \max_{\zeta(t)} \quad & -\sum_{j:k(j) \neq k} \zeta_j(t) \int_0^t G_{kj} \tilde{\mu}_j \eta_j(s) ds \\ \text{s.t.} \quad & \sum_{j:s(j)=i} \zeta_j(t) \leq \Gamma_i, \quad 0 \leq \zeta_j(t) \leq 1. \end{aligned}$$

Which has symmetric dual:

$$\begin{aligned}
& \min_{\beta(t), \gamma(t)} && \sum_i \Gamma_i \beta_{ki}(t) + \sum_i \sum_{j:s(j)=i} \gamma_{kij}(t) \\
& \text{s.t.} && \beta_{ki}(t) + \gamma_{kij}(t) \geq -G_{kj} \tilde{\mu}_j \int_0^t \eta_j(s) ds \quad \forall i, j : s(j) = i \\
& && \beta(t), \gamma(t) \geq 0
\end{aligned}$$

For budgeted uncertainty, our proof uses the same procedure of adding extra variables $w_j(t)$ as the proof of Proposition 2, and creates separate LP subproblems for each server as we did for one-sides. The duals of these have the form:

$$\begin{aligned}
& \min_{\beta(t), \gamma(t), \delta(t), \nu(t)} && \sum_i \Gamma_i \beta_{ki}(t) + \sum_i \sum_{j:s(j)=i} \gamma_{kij}(t) \\
& \text{s.t.} && \delta_{ki}(t) - \nu_{kij}(t) = -G_{kj} \tilde{\mu}_j \int_0^t \eta_j(s) ds \quad \forall i, j : s(j) = i \\
& && \beta_{ki}(t) + \gamma_{kij}(t) - \delta_{kij}(t) - \nu_{kij}(t) \geq 0 \\
& && \beta_{ki}(t), \gamma_{kij}(t), \delta_{kij}(t), \nu_{kij}(t) \geq 0
\end{aligned}$$

From which we combine the two constraints using the substitution $\nu_j(t) = \delta_j(t) + G_{kj} \tilde{\mu}_j \int_0^t \eta_j(s) ds$. This gives the result in Table 2.

For polyhedral uncertainty sets, the single corresponding dual problem is:

$$\begin{aligned}
& \min_{\delta(t)} && \sum_m d_m \delta_m(t) \\
& \text{s.t.} && \sum_m D_{mj} \delta_m = -G_{kj} \tilde{\mu}_j \int_0^t \eta_j(s) ds, \quad \delta(t) \geq 0.
\end{aligned}$$

This gives the result in Table 2.

□